phys. stat. sol.
Subject classification: 61.43.Gt; 78.20.Wc; S7.11

Porous III-V Compounds as Nonlinear Optical Materials

I.M. Tiginyanu[1]) (a), I.V. Kravetsky (a), S. Langa (a),
G. Marowsky (b), J. Monecke (c), and H. Föll (d)

(a) Laboratory of Low-Dimensional Semiconductor Structures, Institute of Applied Physics, Technical University of Moldova, MD-2004 Chisinau, Moldova

(b) Laser-Laboratorium Göttingen e.V., Hans-Adolf-Krebs-Weg 1, D-37077 Göttingen, Germany

(c) Institut für Theoretische Physik, TU Bergakademie Freiberg, Bernhard-von-Cotta-Str. 4, D-09586 Freiberg, Germany

(d) Technische Fakultät, Lehrstuhl für Materialwissenschaft, Christian-Albrechts Universität zu Kiel, Kaiserstr. 2, D-24143 Kiel, Germany

(Received ......**)**

Abstract Electrochemical etching is shown to represent a unique approach for tailoring linear and nonlinear optical properties of III-V compounds. We demonstrate that under defined etching conditions uniformly distributed pores with transverse dimensions less than 100 nm are formed. The presence of pores modifies the refractive index of the materials and, with parallel orientation, induces an artificial optical anisotropy, as evidenced by optical transmission studies. Small dimensions of both pore and skeleton entities are shown to provide the optical homogeneity of the porous specimens. The enhanced optical second harmonic generation (SHG) inherent to porous membranes of GaP containing triangular-prism like pores is attributed to giant third order electric field fluctuations. The dependence of the SHG phase matching angle upon the degree of porosity is deduced.

---

[1]) Corresponding author: phone +373-2247850; Fax: +373-2232252; e-mail: tiginyanu@mail.md

Introduction

It is well known that III-V compounds possess second order nonlinear optical coefficients several orders of magnitude higher than those of KDP, ADP and other materials used infrequency upconversion. However, the utilization of large nonlinear susceptibilities of III-V compounds has not been possible due to high dispersion and lack of birefringence necessary for phase matching [1]. Electrochemistry proves to be a powerful tool for introducing the necessary optical anisotropy in semiconductor materials. Anodically etched Si, for instance, was found to exhibit anisotropy in the infrared region [2]. The measured birefringence (defined as the difference in the effective refractive indices of the electric fields polarized parallel and perpendicular to the pore axis) reaches a maximum value of 0.366 at the wavelength $\lambda = 6.52$ µm [2] which exceeds the birefringence of quartz by a factor of 43. Recently the electrochemical etching techniques were used to fabricate semiconductor sieves of gallium phosphide, i.e., two-dimensionally nanostructured membranes exhibiting a strongly enhanced optical second harmonic generation in comparison with the bulk material [3]. In this work, we study the characteristics of optical transmission and second harmonic generation (SHG) in optically homogeneous and inhomogeneous porous membranes of III-V compounds. We show that enhanced optical nonlinearities accompanied by artificial anisotropy make electrochemically etched III-V compounds promising for advanced nonlinear optical applications.

Experimental Details

N-type (111) oriented InP and GaP wafers cut from Czochralski grown ingots were used in this work. The free carrier concentration was $n = 10^{18}$ cm^{-3} at 300 K. The anodization was carried out in HCl and H_2SO_4 aqueous electrolytes as described elsewhere [3,4]. The area of the sample exposed to the electrolyte was 1 cm^2. The supply of holes was due to the reverse bias applied to the semiconductor/electrolyte junction, which involves the avalanche breakdown effects accompanied by generation of electron-hole pairs. A configuration with four electrodes was used: a Pt reference electrode in the electrolyte, a Pt sense electrode on the sample, a Pt counter electrode, and a Pt working electrode. The electrodes were connected to a specially designed potentiostat/galvanostat, which can deliver currents and voltages up to 200 mA and ± 80 V respectively. The temperature was kept constant at T = 20°C by means of a Julabo F25 thermostat. The electrolyte was pumped continuously by means of peristaltic pumps. All the equipment used in the experiments was computer controlled. The morphology of the porous layers was analysed with a scanning electron microscope (SEM). Special attention was paid to the optimization of the anodic etching conditions leading to the formation of non-cylindrical pores. Scanning electron microscope (SEM) images taken from a porous InP(111) membrane are illustrated in Fig. 1. One can see that most of the pores possesses triangular-prism shape, the lateral size of pores is between 50 nm to 100 nm.

Polarized SHG measurements were carried out in a transmission mode. As a fundamental beam, the 1064 nm output of a Q-switched Nd-YAG laser (Spectra Physics GCR-170) with 10 Hz repetition rate and 7 ns pulse width was used. To minimize the influence of the laser output fluctuations, the measured second harmonic (SH) intensity was normalized by the simultaneously monitored laser intensity in the reference channel. The direction of the fundamental beam polarization was changed by rotating the half-wave plate placed in the front of the sample.

Results and Discussion

Theoretical predictions

In the framework of the effective medium theory a cubic semiconductor with randomly distributed air-filled pores all aligned in z-direction, is considered as a homogeneous uniaxial material with an effective dielectric tensor

$$\bar{\varepsilon}_{ik}\left(\varepsilon^{semic.},\varepsilon^{air},porosity\right) \qquad (1)$$

and an effective non-linear optical tensor

$$\overline{\chi}_{ikl}\left(\chi_{123}^{semic.}, \chi^{air} = 0, porosity\right). \qquad (2)$$

In the case of a (111)-surface the cubic point group T_d is changed to C_{3V} , in which case $\overline{\chi}_{ikl}$ has three independent components $\overline{\chi}_{111}$, $\overline{\chi}_{113}$ and $\overline{\chi}_{333}$ [1]. Following Hui and Stroud [5] $\overline{\chi}_{111}$ e.g. is given by

$$\overline{\chi}_{111} = \chi_{123}^{semic.}\sqrt{6}\left\langle a_2^2 a_1 - \frac{1}{3}a_1^3\right\rangle_{SV}, \qquad (3)$$

where $\langle ... \rangle_{SV}$ is the average $\frac{1}{V_s}\int_{V_S} dV...$ over the volume occupied by the semiconducting material.

The $a_{1,2}(\vec{r})$ are given by

$$a_{1,2}(\vec{r}) = \frac{\partial E_{x,y}(\vec{r})}{\partial E_x^0}, \qquad (4)$$

where $\vec{E}(\vec{r})$ is the electric field inside the sample (calculated in the approximation of the linear medium) and $\vec{E}_0$ is the average over $\vec{E}(\vec{r})$ taken over the total sample volume

$$\vec{E}_0 = \langle E \rangle_V = \frac{1}{V}\int_V dV\vec{E}(\vec{r}) . \qquad (5)$$

The other non-vanishing components of $\vec{\chi}_{ikl}$ have to be calculated from similar formulae, all containing combinations of third order fluctuation terms of the kind $\langle E_i E_k E_l \rangle_{SV}$ divided by products of the kind $E_i^0 E_k^0 E_l^0$.

An enhanced non-linearity, i.e. $\overline{\chi}_{ikl}$ components are much bigger compared to $\chi_{123}^{semic.}$, requires strong third order field fluctuations. By common sense this seems to be unlikely, because fields in a semiconductor material with high dielectric constant are screened,

$$\left\langle \vec{E} \right\rangle_{SV} < \vec{E}_0 . \qquad (6)$$

Likewise it can be proved exactly that $\left\langle \vec{E}^{2} \right\rangle_{SV} < \vec{E}_{0}^{2}$. However, using the special isotropic structure model of Bruggeman [6] for a non-linear metal-insulator composite, Bergman [7] was able to prove that fourth order fluctuations $\left\langle E^{4} \right\rangle_{metal} / E_{0}^{4}$ even can diverge. Repeating this analysis for the dielectric case $\sigma_{I} = 0 \longrightarrow \varepsilon_{1}$, $\sigma_{M} = \longrightarrow \varepsilon_{2}$ with $, \frac{\varepsilon_{2}}{\varepsilon_{1}} \geq 10$ the fourth order fluctuations diverge, too.

These divergences are connected with and due to a so-called percolation threshold, a relative concentration $0 < f_{0} < 1$ at which the σ_{M} - resp. the ε_{2}-material forms connected paths through the sample. All simple structure models without such a percolation threshold do not result in large fourth order fluctuations. The Bruggeman model is based on spherical inclusions of both materials in a self-consistently calculated effective matrix. On the other hand, it is well known, that the fields near sharp edges are much larger than fields near spherical surfaces, therefore we believe that non-spherical inclusions (non-cylindrical pores in our case) can result in large third order fluctuations, too.

Optical characterization

We have studied the linear optical properties of porous membranes to evaluate the material transparency and optical anisotropy. Fig. 2, curve 1, shows the transmission spectrum of a porous InP(111) membrane exhibiting parallel pores with triangular-prism like shape and transverse dimensions less than 100 nm. Note that in this membrane the pores are uniformly distributed and no pronounced fluctuations in their sizes exist (Fig. 1). As one can see from Fig. 2, the optical transmission spectrum of the porous membrane involved shows pronounced interference fringes in the spectral interval corresponding to quantum energies lower than the band gap of bulk InP ($h\nu < E_g = 1.3$ eV). The observation of interference fringes is indicative of optical homogeneity of the porous medium. Due to the relatively small dimensions of both pore and skeleton entities, the porous medium proves to be optically homogeneous, and therefore the light propagates through it without pronounced scattering. In case of a non-uniform distribution of pores the membranes become optically inhomogeneous which leads to pronounced light scattering and decreases in transparency (Fig. 2, curve 2). Similar results have been obtained for porous GaP membranes (Fig. 3).

In optically homogeneous porous membranes the degree of porosity defines the optical anisotropy caused by the preferential orientation of pores along the <111> crystallographic direction. According to the effective medium theory [8], in the case of pores stretching perpendicular to the initial surface, the components of the dielectric tensor of the porous membrane can be written as follows:

$$\varepsilon_{//}(\omega) = (1-c)\varepsilon_1 + c\varepsilon(\omega), \qquad (7a)$$

$$\varepsilon_{\perp}(\omega) = \varepsilon(\omega)\frac{\varepsilon_1\cdot(2-c)+c\cdot\varepsilon(\omega)}{\varepsilon_1\cdot c+\varepsilon(\omega)\cdot(2-c)} \qquad (7b)$$

where c is the concentration of semiconductor material, $\varepsilon(\omega)$ is the dielectric function of the III-V compound, and ε_1 is the dielectric constant of air. Due to $\varepsilon_{\perp}(\omega)<\varepsilon_{//}(\omega)$ for all c, the porous semiconductor represents a positive uniaxial material.

Fig. 4 shows the transmission of light with λ = 1064 nm by a porous membrane with the thickness 8.2 μm as a function of the incident angle of the laser beam. The position of the maxima displayed by the interference patterns depends upon the direction of light polarization. For the ordinary beam, the maxima occur at incidence angles of 17 and 43 degrees, while for the extraordinary beam the maxima occur at 21 and 49 degrees. The analysis of the interference conditions for the two beams taking into account Eqs. (7a) and (7b) allows one to calculate the refractive indices: n_o = 2.43 and n_e = 2.67. Evidently, the porous membranes exhibit pronounced birefringence necessary for phase matching in optical second harmonic generation.

Fig. 5 illustrates the transmitted s-polarized second harmonic signals ($\lambda_{2\omega}$ = 532 nm) from both bulk (111)-oriented GaP and a porous membrane as a function of the incident angle of the s-polarized fundamental beam. Despite of the short coherence length ($L_{\mathrm{coh}} \sim 1$ µm) it is not possible to see Maker fringes in GaP because of a sufficiently high absorption at the SH frequency [9]. The pronounced absorption at 2ω is caused by the fact that the corresponding energy is higher than the indirect band gap of GaP ($2\hbar\omega > E_g = 2.24$ eV). As one can see from Fig. 5, under identical conditions the porous membranes exhibit a SH intensity of at least two orders of magnitude higher than that inherent to bulk GaP. Another interesting feature is that the fundamental incident angle dependence of the SH intensity for porous membranes measured in s-s polarization geometry shows pronounced shoulders at – 35 and + 35°.

Fig. 6 (solid squares) illustrates the rotational dependence of the second harmonic intensity for an optically homogeneous porous GaP(111) membrane possessing triangular-prism like pores. It reflects perfectly the crystallographic features of (111)-oriented GaP demonstrating the high crystalline quality of the porous skeleton. On the contrary, optically inhomogeneous GaP membranes reflect no crystallographic features of the semiconductor compound (Fig. 6, solid triangles) since in the case of strong diffuse scattering any dependence of the SHG signal upon the rotation angle of the porous membrane about the surface normal is removed.

In optical SHG type I phase matching is achieved if $n_0(2\omega) = n_{e0}(\omega)$, where

$$n_0(\omega) = \sqrt{\varepsilon_\perp(\omega)}, \quad n_{e0}(\omega) = \sqrt{\varepsilon_{e0}(\omega)} \tag{8a}$$

with
$$\frac{1}{\varepsilon_{e0}(\omega)} = \frac{\cos^2\vartheta}{\varepsilon_\perp(\omega)} + \frac{\sin^2\vartheta}{\varepsilon_{//}(\omega)} . \tag{8b}$$

ϑ is the angle between the optical axis and the exciting laser beam inside the membrane. Taking into account that $\varepsilon_1 = 1$, $\varepsilon(\omega) = 3.1192^2$ and $\varepsilon(2\omega) = 3.4595^2$ [1], one can solve the equation $n_0(2\omega) = n_{e0}(\omega)$ in order to determine ϑ as a function of c. A solution exists for all $c < 0.696$, it means for the degree of porosity $(1 - c) \geq 30$ %. The dependence of the phase matching angle as a function of the GaP concentration is illustrated in Fig. 7. Note that membranes with 30 % porosity fulfill the phase matching conditions provided that the fundamental and SH beams propagate in directions that are nearly perpendicular to the pores. So, it is possible to elaborate integrated optoelectronic structures where specially designed porous III-V layers play the role of both waveguides and frequency upconverters.

Conclusions

Porosity-based technological approaches prove to be very important for elaborating new nonlinear optical elements ready to be integrated in optoelectronic circuits. First, the formation of pores leads to symmetry breaking. In particular, pores parallel to the <111> direction in III-V compounds change the cubic crystal symmetry (point group T_d) to the uniaxial trigonal one (point group C_{3v}). The porosity-induced artificial birefringence opens the possibility to meet the phase matching conditions for the second harmonic generation in III-V materials. For gallium phosphide, in particular, the phase matching conditions can be fulfilled for degrees of porosity higher than 30 %. Second, porous structures represent heterogeneous media where the electric field undergoes large spatial variations. Especially strong local field fluctuations are expected in structures containing pores with sharp edges, e.g., triangular-prism like pores. Porous GaP membranes with triangular-prism like pores exhibit a SHG efficiency two orders of magnitude higher than that of bulk material. In spite of the electric field screening in the semiconductor, the third order field fluctuations responsible for the SHG enhancement seem to be giant in case of pores with sharp edges. Taking into account existing theories, an important role in the SHG enhancement may be attributed to the material percolation which is responsible also for the mechanical stability and good thermal conductivity of porous membranes.

It is interesting to note that new nonlinear optical media can be created just by filling in the pores in porous III-V compounds with other materials. In this case the semiconductor skeleton can be designed to provide phase matching while the material filling the pores will contribute mainly to the SHG. Note that porous III-V compounds as phase-matching matrices are much more promising than elementary semiconductors due to their larger band gap and their more pronounced anisotropy when subjected to electrochemical etching.

Acknowledgements This work was supported by the Deutsche Forschungsgemeinschaft (DFG) under the grants No 436 MOL 113/1/0-1, 436 MOL 113/2/0-1 and FO 258/4-1.

Figure captions

Fig. 1. SEM images taken from a porous InP membrane: a) top view; b) cross-section view.

Fig. 2. Transmission spectra of optically homogeneous (curve 1) and inhomogeneous (curve 2) porous InP membranes.

Fig. 3. Transmission spectra of optically homogeneous (curve 1) and inhomogeneous (curve 2) porous GaP membranes.

Fig. 4. Transmission of light with λ = 1064 nm by a porous GaP membrane as a function of the incident angle of the laser beam measured in q-s and q-p polarization geometries.

Fig. 5. Measured s-polarized SH intensity as a function of the incident angle of the s-polarized fundamental beam for bulk and porous GaP.

Fig. 6. SH intensity induced by a 1064 nm polarized pump beam at normal incidence as a function of the azimuthal rotation angle of the optically homogeneous (solid squares) and inhomogeneous (solid triangles) porous GaP membranes measured in parallel polarization. The solid line is a fit.

Fig. 7. Dependence of phase matching angle for optical SHG in porous membranes upon the GaP concentration.

Figure 1.

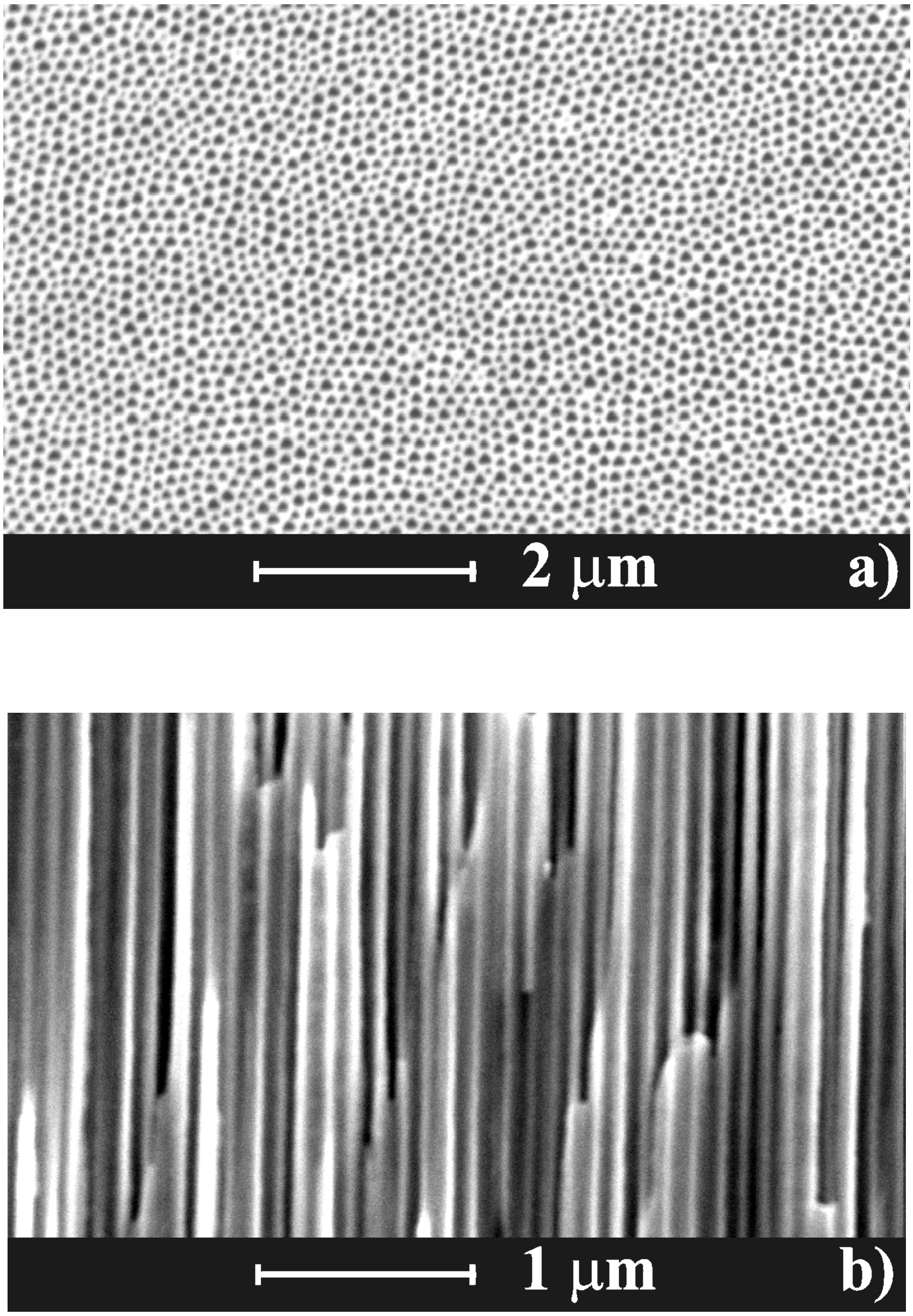

Figure 2.

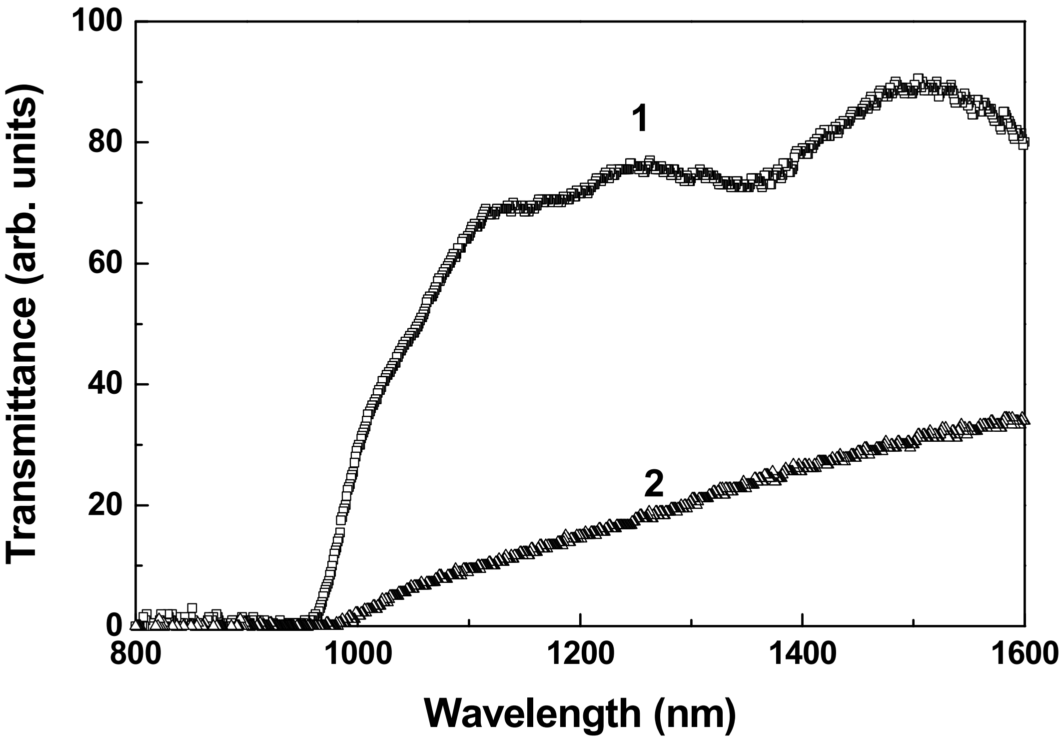
100
80
60
40
20
0
800
1000
1200
1400
1600
Transmittance (arb. units)
Wavelength (nm)
1
2

Figure 3.

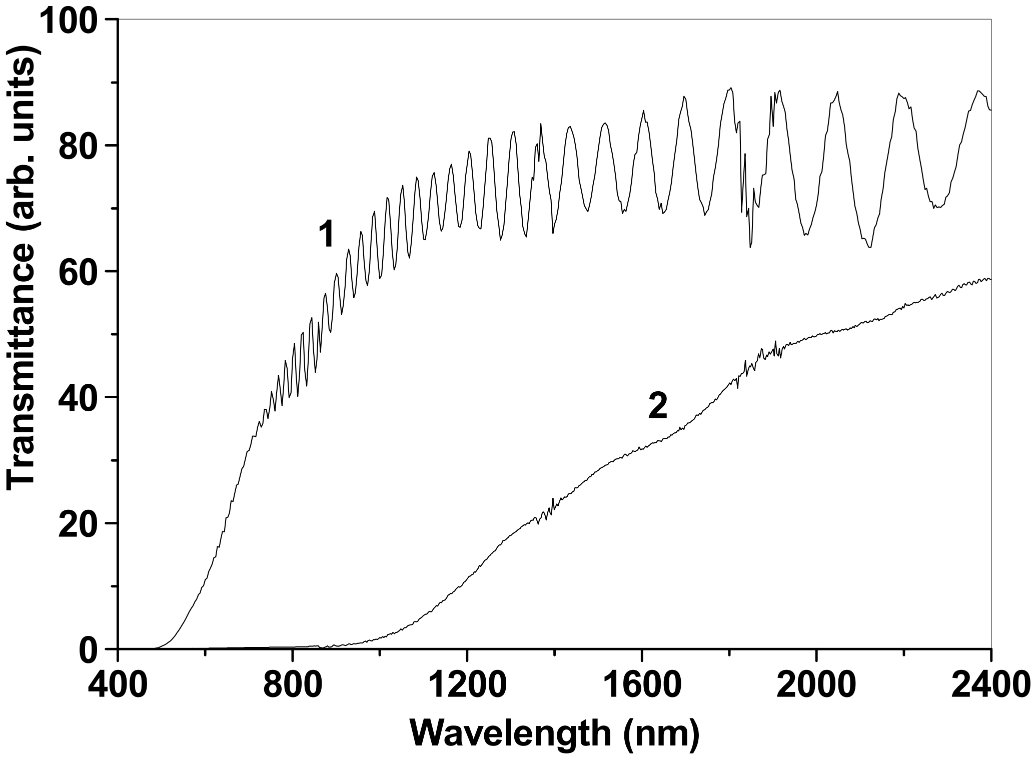
100
80
60
40
20
0
Transmittance (arb. units)
400
800
1200
1600
2000
2400
Wavelength (nm)
1
2

Figure 4.

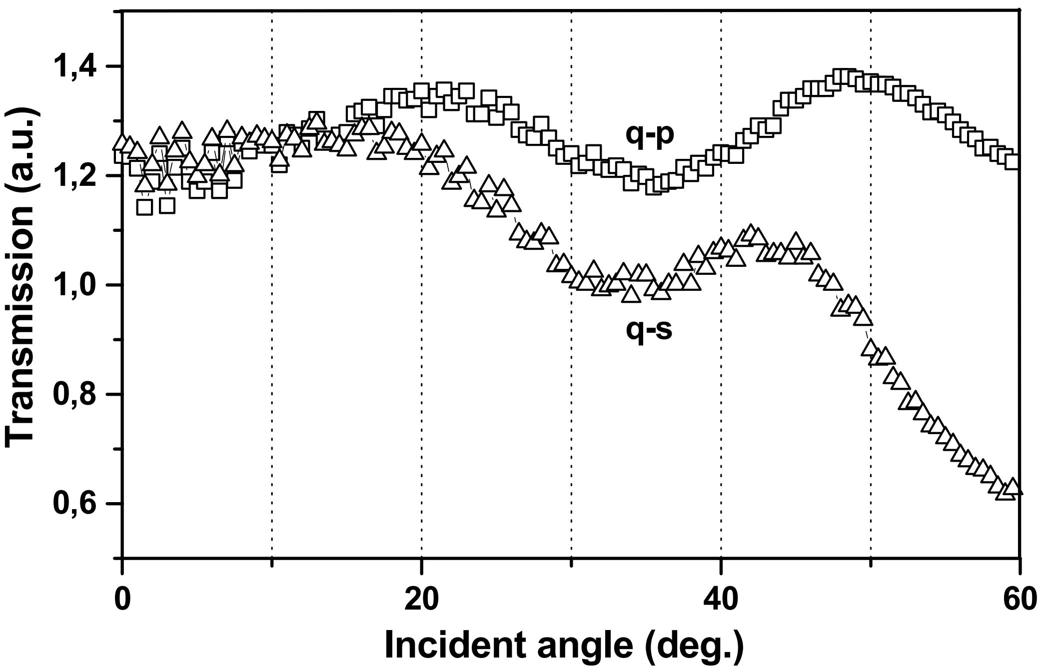
1,4
1,2
1,0
0,8
0,6
Transmission (a.u.)
0
20
40
60
Incident angle (deg.)
q-p
q-s

Figure 5.

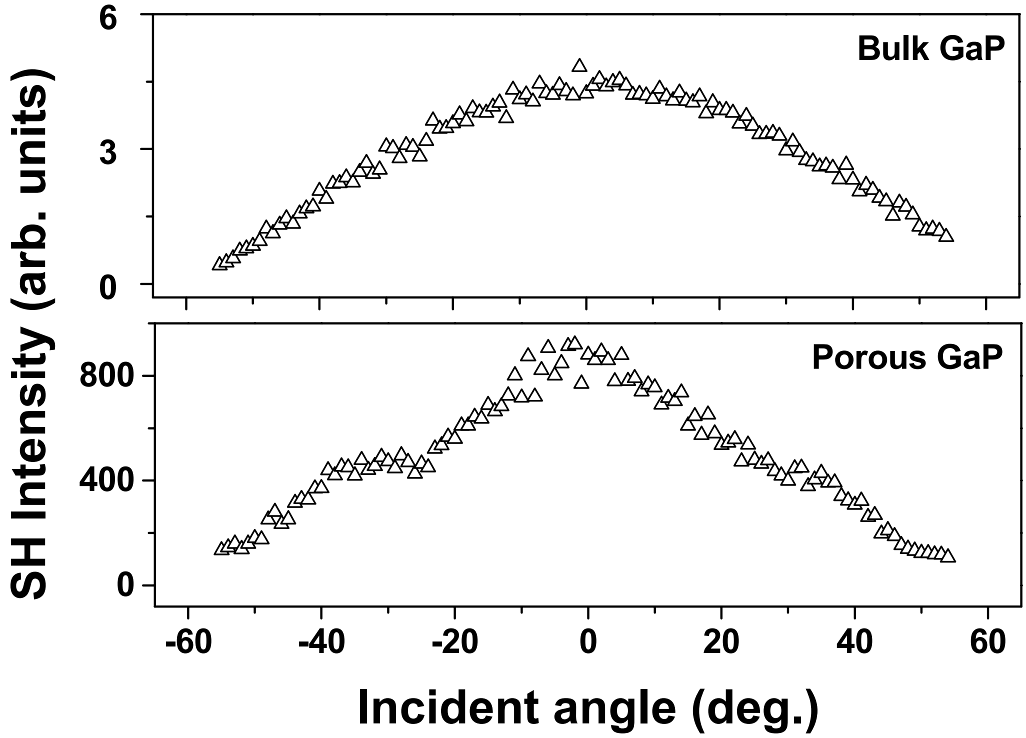

SH Intensity (arb. units)
6
3
0
Bulk GaP
800
400
0
Porous GaP
-60
-40
-20
0
20
40
60
Incident angle (deg.)

Figure 6.

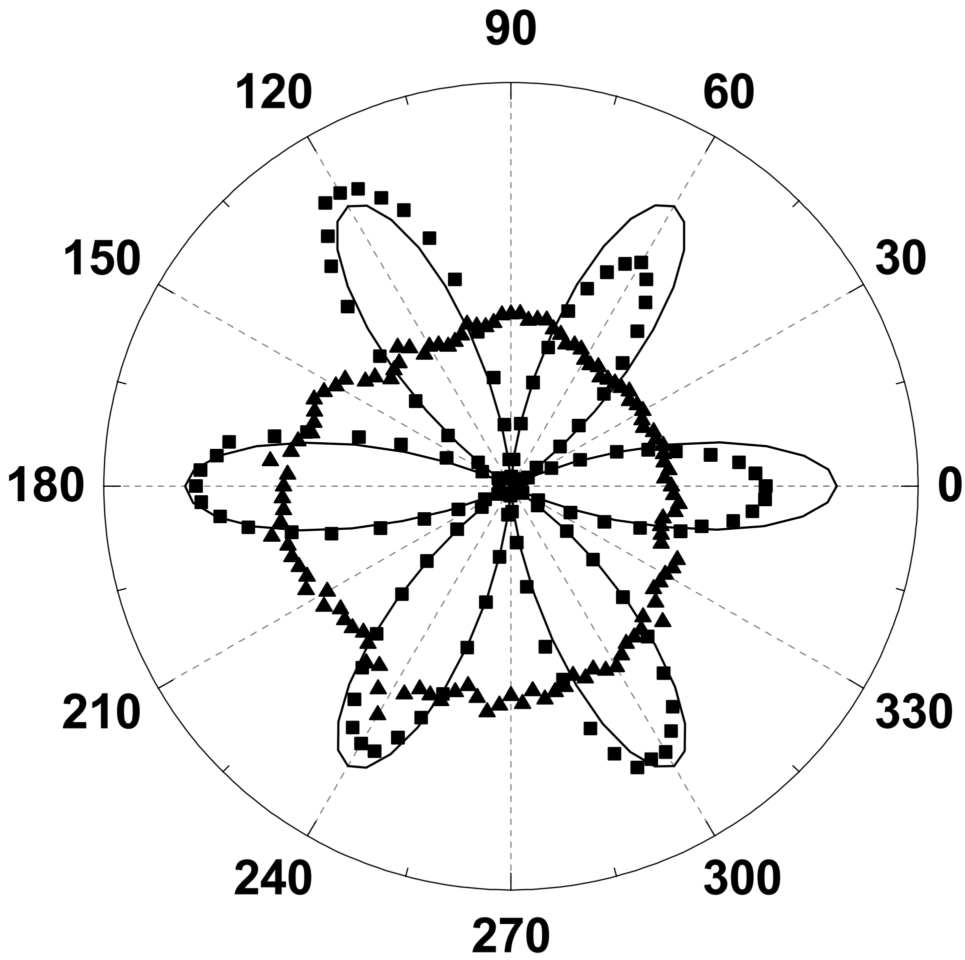

Figure 7.

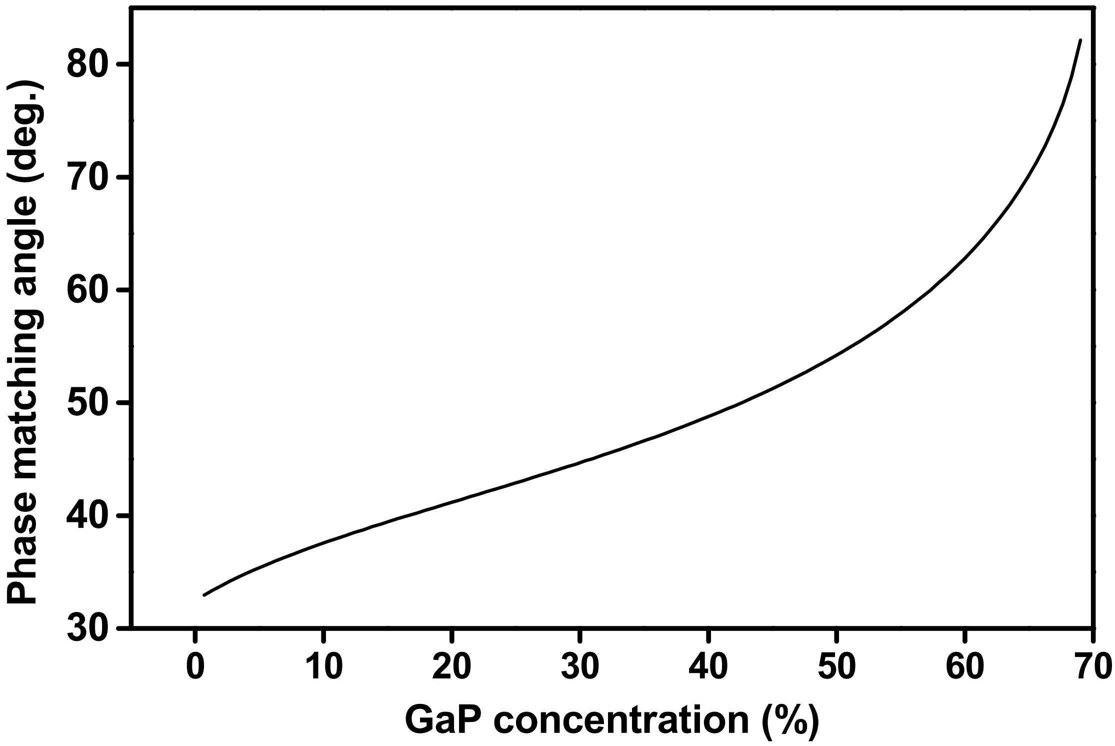
Phase matching angle (deg.)
30
40
50
60
70
80
0
10
20
30
40
50
60
70
GaP concentration (%)

References

[1] S. Singh, in: Handbook of Lasers with Selected Data on Optical Technology, Ed. R.J. Pressley, Chemical Rubber CO, Cleveland, Ohio 1971 (p. 504).

[2] F. Genereux, S.W. Leonard, H.M. van Driel, A. Birner, and U. Gösele, Phys. Rev. B **63**, 161101 (2001).

[3] I.M. Tiginyanu, I.V. Kravetsky, J. Monecke, W. Cordts, G. Marowsky, and H.L. Hartnagel, Appl. Phys. Lett. **77**, 2415 (2000).

[4] S. Langa, J. Carstensen, M. Christophersen, H. Föll, and I. M. Tiginyanu, Appl. Phys. Lett. **78**, 1074 (2001).

[5] P.M. Hui, and D. Stroud, J. Appl. Phys. **82**, 4740-4743 (1997).

[6] D.A.G. Bruggeman, Ann. Phys. Lpz. **24**, 636-679 (1935).

[7] D.J. Bergman, Phys. Rev. B **39**, 4595-4609 (1989).

[8] D.J. Bergman, Phys. Rep. **43**, 377 (1978).

[9] W.N. Herman, and L.M. Hayden, J. Opt. Soc. Amer. B **12**, 416 (1995).